LIMNOLOGY
and
OCEANOGRAPHY

ASLO

Limnol. Oceanogr. 9999, 2020, 1–19

doi: 10.1002/lno.11574

Kelp deposition changes mineralization pathways and microbial communities in a sandy beach

Marit R. van Erk,[1*] **Dimitri V. Meier**,[1,a] **Timothy Ferdelman**,[1] **Jens Harder**,[1] **Ingeborg Bussmann**,[2] **Dirk de Beer**[1]

[1]Max Planck Institute for Marine Microbiology, Bremen, Germany
[2]Alfred Wegener Institute, Helmholtz Centre for Polar and Marine Research, Helgoland, Germany

Abstract

We investigated the impact of kelp deposition on the geochemistry and microbial community composition of beach sands on the island of Helgoland (North Sea). The composition of the microbial community at a beach with regular kelp deposition appeared shaped by this regular input of organic material, as indicated by significantly higher proportions of aerobic degraders, fermenters, and sulfur cycling microorganisms. Rapid degradation of deposited kelp by this community leads to high levels of dissolved organic and inorganic carbon and nutrients, a lower pH and anoxia. Aerobic respiration, fermentation, Fe- and SO_4^{2-} reduction, and methanogenesis were strongly enhanced, with SO_4^{2-} reduction being the main process in kelp degradation. SO_4^{2-} reduction rates increased 20- to 25-fold upon addition of kelp. The main route of electrons from kelp to SO_4^{2-} was not via CO and H_2, as expected, but via organic fermentation products. O_2 supply by the tides was not sufficient and reduced intermediates escaped from the sediment with tidal water retraction. The resulting extremely high levels of free sulfide (>10 mmol L^{-1}) lead to abundant filamentous growth of sulfur-oxidizing bacteria largely composed of a rare O_2-adapted *Sulfurovum* lacking the expected denitrification genes. Our results show that regular kelp deposition strongly enhances the thermodynamic disequilibrium in the beach sand habitat, leading to a dramatic enhancement of the sulfur cycle.

Large amounts of organic material consisting mainly of macroalgae and seagrasses are regularly deposited on shores. Kelps, or brown macroalgae, need a hard substrate on which to attach, and occur along all temperate shores (Mann 1973). Kelp beds can attain high rates of production and form a large pool of biomass (Mann 1973). Physical forcing of storms and waves causes the sessile kelp plants to become detached. The detached kelp may subsequently be carried ashore, and form layers of up to several meters thick on shores nearby rocky seafloors. Rates of annual kelp deposition were estimated to be between 1.2×10^6 and 1.8×10^6 kg wet weight along a 1 km strandline in South Africa (Koop and Field 1980). Such large accumulations of organic material in the marine realm are sporadic but locally dramatic, and the sequence of events that follows sudden pulses of organic material is complex and of great interest to microbial ecologists and biogeochemists. Another example of such a pulse biogeochemical impact is the arrival of a whale carcass on the sea floor (Treude et al. 2009). Such an input of degradable organic material results in unusually high levels of organic substrates, intermediates, and degradation products. Degradation will depend on arrival of and colonization by degrading organisms, transport rates of degradation products, and the period the organic material resides in the habitat (i.e., relocation of kelp by tides).

Macroalgal deposits on beaches are classified as biogeochemical hotspots as they are metabolically very active, with high CO_2 fluxes demonstrating elevated respiration rates (Rodil et al. 2019). Studies focusing on the effects of increased amounts of organic material within sandy sediments found surface sediments to be anoxic, and dissolved reduced sulfur concentrations and SO_4^{2-} reduction to be enhanced (Böttcher et al. 1997). This further highlights the enhanced metabolic activity of sandy sediments characterized by large depositions of organic material.

Kelp deposits are a source of dissolved organic carbon (DOC) and nutrients. The release of leachates to the sediments was shown by high concentrations of DOC in associated sediments, exceeding concentrations in offshore kelp beds. The released DOC can be used rapidly within the sediments (Koop

*Correspondence: merk@mpi-bremen.de

Additional Supporting Information may be found in the online version of this article.

[a]Present address: Division of Microbial Ecology, Centre for Microbiology and Environmental Systems Science, University of Vienna, Vienna, Austria

et al. 1982). Mineralization of kelp detritus on beaches leads to the export of nutrients to the sea. A significant correlation between intertidal dissolved inorganic and organic nitrogen (DIN and DON) concentrations and deposit biomass was found (Dugan et al. 2011). These authors also found DIN concentrations in surf zone waters to correlate with deposit biomass and intertidal DIN concentrations, suggesting that deposits cause the release of DIN to the sediments, which is subsequently partly exported to the surf zone water. Beaches with kelp deposits could therefore be important sites of biogeochemical activity for nearshore communities (Dugan et al. 2011).

Sandy beach sediments are characterized by low contents of organic material compared to muddy sediments (Jickells and Rae 1997), and heterotrophic organisms within sandy beach sediments are thus dependent on the input of allochthonous organic material. Kelp-derived carbon was found throughout nearshore food webs (Duggins et al. 1989). Besides being a food source, kelp deposits provide a habitat and shelter against predation and environmental conditions to a variety of organisms (Colombini et al. 2000). Deposits increase the density and species richness of communities (Colombini and Chelazzi 2003). Invertebrate consumers fragment the kelp material and thereby make the material available to bacteria (Colombini and Chelazzi 2003).

Bacteria are the key decomposers of the kelp deposits and the further mineralization occurs via a complex set of microbial processes. Kelp dry biomass is rich in polysaccharides, such as alginic acid, laminarin, mannans, and fucoidan (Usov et al. 2001). Therefore, degradation likely involves the hydrolysis of polymers, fermentation of hydrolysis products, and aerobic and anaerobic oxidation processes. The largest fraction of biomass associated with kelp deposits is microbial, being about three times that of macro- and meiofauna (Koop and Griffiths 1982). Over 90% of the kelp-derived leachates is used by bacteria, and a large fraction (23–27%) of kelp carbon is converted to bacterial carbon, with the remainder rapidly being mineralized by bacteria (Koop et al. 1982). A positive relationship between DIN concentrations below deposits and bacterial diversity further supports the role of bacteria as key decomposers of the deposits (Rodil et al. 2019). Remarkably, no detailed biogeochemical studies on degradation within kelp deposits on sandy beaches, including analyses on the release of substances, microbial processes, and associated microbial communities, have been performed. Here, we report on such a study carried out on a North Sea beach.

We hypothesize that the microbial communities associated with kelp deposits are different from the normal coastal communities within sandy intertidal sediments. In normal early diagenesis, mass transfer of organic material and electron acceptors to the cells limits turnover rates, as advectional exchange of electron acceptors between oxygenated seawater (the source of electron acceptors, e.g., O_2, NO_3^-, SO_4^{2-}) and sediment is limited. This leads to a vertical stratification of processes, the redox cascade, in a typical sequence of electron acceptors (O_2, NO_3^-, Mn(IV), Fe(III), SO_4^{2-}, and CO_2) dictated by the energy gain related to the different processes (Froelich et al. 1979). The reduction processes are coupled to reoxidation of the reduced products (Berner 1980). In general, microorganisms in early diagenesis are limited by one or several compounds, and microbial communities are thus thought to be specialized in slow growth and to have a high affinity to limiting substrates (Chen et al. 2017). SO_4^{2-} reduction is an important process in marine sediments, as it can account for 50% of the remineralization of organic material in coastal sediments (Jørgensen 1982).

Conditions in sediments below kelp deposits are expected to be different from steady-state depositional environments. Mineralization processes after sudden inputs of large amounts of organic material are ultimately controlled by kinetics, which in turn depend on the presence of the optimal microbial consortia, substrate quality, pH, temperature, and other microenvironmental factors. The batch-wise input of a large amount of readily degradable material will favor fast-growing organisms, and leads to high levels of intermediates, e.g., fermentation products. The short deposition time may favor facultative anaerobes, but not allow for full development of the anaerobic processes that are common in diffusion-controlled sediments.

An interesting route for stimulating SO_4^{2-} reduction could be via the intermediates CO and H_2. Formation of CO occurs from organic material, likely polyphenols, under oxic conditions by abiotic processes (Conrad and Seiler 1985). The formation of CO in intertidal environments is thus likely an aerobic process. CO can biologically react with water to produce H_2: $CO + 2H_2O \rightarrow HCO_3^- + H_2 + H^+$ (Parshina et al. 2010). The produced H_2 could be an important substrate for SO_4^{2-} reduction. This is a possible scenario in the intertidal zone with fluctuating O_2 conditions. Alternatively, CO can be used directly as electron donor in SO_4^{2-} reduction.

Sandy beaches consist of permeable sediments in which advection plays a major role. Advection efficiently transports organics and electron acceptors from the water column into the sediments, however, only by hydraulic forcing.

We investigated the hypotheses that the degradation rates are strongly enhanced and degradation follows other pathways than on beaches without kelp. Specifically, we expected that CO and H_2 may be important intermediates, and export from the sediments of intermediates and products of anaerobic processes occurs. The hypotheses were tested using porewater and sediment analyses, radiotracer (^{35}S) incubations and in situ microsensor measurements, as well as microbial community composition analysis and selective population-resolved genomic potential analysis.

Materials and methods

Site description

Helgoland is a small archipelago in the German Bight, southeast North Sea (54°11′ N; 7°53′ E). It lies approximately

60 km off the German coast and consists of two islands: the main island (Hauptinsel) to the west (1 km^2) and the smaller Düne to the east (0.7 km^2). The tidal regime of Helgoland is semidiurnal, with an average tidal range of 2.3 m. Around Helgoland, the sublittoral hard-bottom sediment is covered by brown seaweeds: mainly *Laminaria digitata*, *Laminaria hyperborea*, *Saccharina latissima*, and *Desmarestia aculeata* (Pehlke and Bartsch 2008), of which the first three are kelp species, and have leaves that are up to over a meter in length. Two sandy beaches on the main island were selected as sampling locations: the North Beach, hereafter referred to as kelp-beach, and a reference beach (Fig. 1). An area of 1 km^2 of the kelp forest is located north of the kelp-beach (Uhl et al. 2016), the main source for huge masses of kelp deposits on this beach. Deposition happens often but irregular, with highest deposition rates occurring during and directly after storms. Sampling for biogeochemical analyses was conducted in November 2017, May 2018, October 2018, and August 2019 (Table 1), during low to incoming tide in water-saturated sediments. The microbial community composition was assessed using samples obtained in October 2015, and total cell counts were determined from July 2019 samples.

Sediment properties

Sediments for porosity, total organic carbon (TOC), and solid-phase Fe determinations were sampled in situ using cut-off syringes. Sampling was conducted within the upper 10 cm, in 2 cm intervals. Sediments for TOC determination were freeze-dried, and sediments for Fe determination were stored at −20°C. Sediment density was determined from the wet weight of a known volume of sediment. Porosity was calculated using the weight loss upon drying to constant weight at 60°C. For TOC determination, freeze-dried sediments (0.5–1.0 g) were ground and homogenized. Sediments were then decalcified using 10% HCl, and freeze-dried. The TOC concentration was determined in duplicate on 40–50 mg of sediment using a continuous-flow elemental analyzer (Thermofinnigan Flash EA 2000) coupled to an isotope ratio mass spectrometer (Delta V plus). For solid-phase Fe(III) and Fe(II) determination, Fe was extracted from about 0.5 g of wet sediment using 5 mL of 0.5 mol L^{-1} HCl (0.5 h). Supernatants were then analyzed spectrophotometrically using the ferrozine method (Viollier et al. 2000).

Porewater extraction and analysis

Porewater extraction and filtration were conducted in the field using Rhizon samplers (Rhizosphere Research Products, average pore size 0.15 μm). Sampling was conducted in 2 cm intervals from 0 to 12 cm depth (kelp-beach November 2017), 0 to 14 cm depth (reference beach November 2017), and 0 to 10 cm depth (May and October 2018). In November 2017, extracted kelp-beach porewater at 10 and 12 cm depth was only sufficient for DOC analyses. The first mL of porewater was discarded. Seawater was collected in 50 mL tubes and Rhizon sampling was conducted from these tubes as described for porewater sampling. After extraction and filtration,

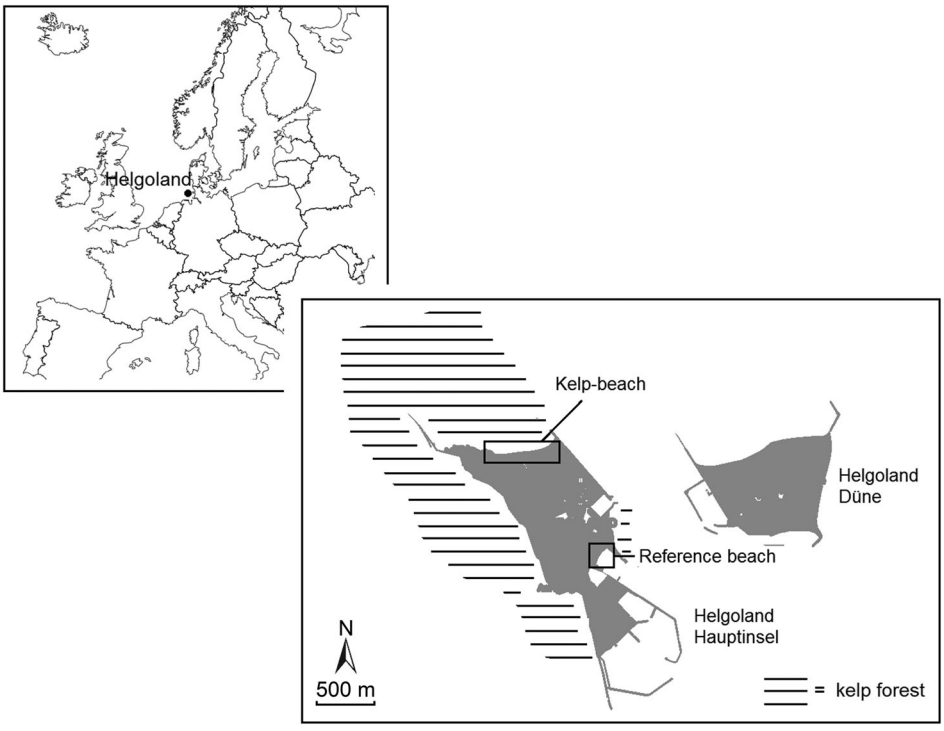

Fig. 1. Location of the two study sites (kelp-beach and reference beach), including the location of the kelp forest (Uhl et al. 2016).

Table 1. Parameters measured during the different field campaigns. Crosses (X) denote that measurements were done during that campaign. Dashes (—) denote that measurements were not done during that campaign or that data is not shown. TOC, Total organic carbon; DOC, Dissolved organic carbon; P_i, Inorganic phosphorus; DIC, Dissolved inorganic carbon; $S^{2-}{}_{tot}$, Total sulfide; SRR, $SO_4{}^{2-}$ reduction rate.

Parameter	November 2017	May 2018	October 2018	August 2019
Sediment parameters				
Porosity	—	—	X	—
TOC	—	—	X	—
Fe(III) and Fe(II)	—	—	X	—
Porewater parameters				—
DOC	X	—	—	—
Nutrients ($NO_3{}^- + NO_2{}^-$, $NH_4{}^+$, P_i)	X	X	—	—
DIC	—	—	X	—
$SO_4{}^{2-}$	—	X	—	—
Sulfide	—	X	—	—
Cl^-	—	X	—	—
Fe^{2+}	—	—	X	—
Microsensor parameters				—
O_2	—	X	—	—
pH	—	X	—	—
$S^{2-}{}_{tot}$	—	X	—	—
Gases			—	—
CH_4	—	X	—	—
N_2O	—	X	—	—
CO	X	X	—	—
H_2	X	X	—	—
Rates and fluxes				—
SRR	—	—	X	—
O_2 flux/O_2 consumption	—	X	—	X

porewater was directly subsampled from the syringe using a sampling cup attached to the side-outlet of a 3-way stopcock that was between the syringe and the Rhizon sampler. Porewater was transferred to combusted glass vials for DOC and to centrifuge tubes for nutrient ($NO_3{}^- + NO_2{}^-$, $NH_4{}^+$, and inorganic phosphorus [P_i]) determinations. Both the glass vials and centrifuge tubes were stored at −20°C. For dissolved inorganic carbon (DIC) determination, 2 mL glass vials (Zinsser Analytic) were filled without headspace, and stored at 4°C. Porewater was fixed with ZnAc in Eppendorf tubes and stored at 4°C for sulfide, $SO_4{}^{2-}$, and Cl^- determination. For Fe^{2+} determination, porewater was fixed using ferrozine in semimicro cuvettes and stored at 4°C.

Concentrations of DOC were measured by high temperature catalytic oxidation using a DIMATOC® 2010 K1 analyzer, with potassium hydrogen phthalate as standard. Nutrients were analyzed photometrically with a continuous-flow analyzer (BQuAAtro39 analyzer, Seal Analytic), using a variant of a method described previously (Grasshoff et al. 1999). The DIC concentrations were determined using a flow injection system (Hall and Aller 1992). Both $SO_4{}^{2-}$ and Cl^- concentrations were determined by ion chromatography (Metrohm 930 Compact IC Flex). Dissolved sulfide (H_2S, HS^-, S^{2-}) was analyzed spectrophotometrically using the methylene blue method (Cline 1969). The Fe^{2+} concentrations were determined spectrophotometrically within 3 d after sampling using the ferrozine method (Viollier et al. 2000).

Microsensor measurements

Depth profiles were measured in situ at different locations on the kelp-beach and the reference beach. Microsensors for O_2, pH, and H_2S were mounted on a manually operated micromanipulator attached to a heavy stand. The readings were made directly from the displays of the battery-powered amplifier (H_2S, pH) or from the laptop (O_2). Measurements were conducted in water-saturated sediments. Measurements could only be done at low tide or during the first minutes upon inundation. The sites on the kelp-beach were exposed during low tide for approximately 8 h d^{-1}.

O_2 was recorded using micro-optodes (OXROB10, Pyroscience GmbH, Germany), connected to a FirestingO_2 meter (Pyroscience GmbH, Germany) and a laptop with the Pyroscience software. The sensors were calibrated using 1 mol L^{-1} Na ascorbate solution (0% saturation) and

air-saturated water (100% saturation) and signals were corrected for temperature and salinity to calculate the O_2 concentrations. Salinity was measured using a refractometer. The H_2S microsensors were prepared as described previously (Jeroschewski et al. 1996). The multiple-point calibration was conducted in the on-site laboratory by stepwise addition of known amounts of a 1 mol L^{-1} Na_2S solution to acidified (pH < 2) seawater. The steel needle enforced pH microsensors, obtained from Microelectrodes Inc (Bedford, USA), were calibrated in standard buffers. The pH and H_2S concentrations were used to calculate total sulfide (S^{2-}_{tot}) as described previously (Jeroschewski et al. 1996), using a pK of 6.6 or 6.7, depending on the in situ porewater temperature and seawater salinity (Millero et al. 1988).

The diffusive O_2 fluxes were calculated from the O_2 gradients using Fick's first law of one-dimensional diffusion. The effective diffusion coefficient (D_e) of O_2 in the sediment was obtained by multiplying the molecular diffusion coefficient of O_2 (D_0) with the porosity of the sediment (Kühl et al. 1996). The D_0 was corrected for the in situ porewater temperature and salinity (Li and Gregory 1974). For kelp-beach sediments, D_e was equal to 5.04×10^{-10} m^2 s^{-1}, and for reference beach sediments, D_e was equal to 4.68×10^{-10} m^2 s^{-1}.

Volumetric O_2 consumption rates were determined by percolating oxygenated seawater through kelp-beach and reference beach sediments. Surface sediments and seawater were sampled in August 2019 on both beaches, and stored cooled at 4°C until use within 3 d after sampling. Sediments were homogenized and large pieces of kelp and large grains were removed by sieving. The homogenized sediments were carefully added to sediment cores (5.3 cm diameter) that were filled with seawater. The bottom stopper of the core was fitted with a valve. Porewater O_2 concentrations were tracked with O_2 micro-optodes positioned at 2 cm depth. Approximately 50 mL of aerated seawater was percolated through the sediments by outflow through the valve. The sediment cores contained sufficient seawater to allow for a layer of overlying seawater to remain after percolation. An air pump induced continuous water movement in this overlying layer of seawater. The O_2 decrease after percolation was used to calculate the volumetric O_2 consumption rate. Conversion from volume of porewater to volume of sediment occurred by multiplication with the sediment porosity. To determine the areal O_2 consumption rate, the volumetric rate was multiplied with the in situ O_2 penetration depth measured in May 2018 (kelp-beach low tide = 0 cm; kelp-beach incoming tide = 0.8 cm; reference beach = 3.6 cm).

Gas analysis

Sediment was collected in situ using cut-off syringes. Sampling was conducted to a depth of 10 cm, in 2 cm intervals. For CH_4 and N_2O analysis, 3 mL of sediment was transferred to a serum vial containing 3 mL 5 mol L^{-1} NaOH. Serum vials were closed with a butyl rubber stopper and aluminum crimp seal, shaken, and stored at 4°C. Headspace CH_4 and N_2O concentrations were analyzed with a gas chromatograph (GC 2014, Shimadzu) equipped with a flame ionization detector (FID) for CH_4 and an electron capture detector (ECD) for N_2O. Calibration was done with 2, 10, and 100 ppm standards (Air Liquide) for CH_4 and with 1 and 5 ppm standards (Microsense, Denmark) for N_2O. For CO and H_2 analysis, 0.5 mL of sediment was transferred to Exetainers (November 2017) or to Exetainers containing 0.5 mL 20% (w/v) $ZnCl_2$ (May 2018). Samples for CO and H_2 analysis were shaken and analyzed within 3 h by gas chromatography (Peak Performer 1 RCP 910-Series). Calibration was done with 20 and 100 ppm standards (Air Products) for CO and with 100 and 500 ppm standards (Air Products) for H_2.

CO, H_2, and O_2 evolution in experiments

Two 100 mL serum vials were filled with 10 mL of artificial seawater (pH 8.2, salinity 32) and equilibrated to the incubation temperature of 15°C. Pieces of 1 × 1 cm from the middle of *Laminaria hyperborea* leaves were cut out, and about 5 g of these pieces were added to each vial, which were then closed with a butyl rubber stopper and aluminum crimp seal, and incubated in the dark on a horizontal shaker. At selected time points, headspace samples for CO and H_2 analysis were taken using a gas and pressure tight syringe and were directly measured (see above). During incubation, the pressure inside the vials changed as the withdrawal of aliquots was not replaced. Headspace O_2 concentrations were measured continuously using Oxygen Sensor Spots (OXSP5, Pyroscience GmbH) glued to the inner side of the vial. The sensor spots were calibrated using a 2-point calibration with N_2 gas (0%) and O_2-saturated air (100%). Only O_2 concentrations from the time points at which CO and H_2 sampling was conducted are shown.

SO_4^{2-} reduction rates

SO_4^{2-} reduction rates within kelp-beach and reference beach sediments

The SO_4^{2-} reduction rates (SRR) were determined on 3 mL sediment samples that were collected using cut-off syringe cores, in 2 cm intervals, from 0 to 10 cm depth. On the kelp-beach, sediments were sampled both below and next to kelp deposits. Syringe cores with sediments were transported cooled and in the dark to the laboratory. There, ^{35}S tracer was added to anoxic seawater, and 3 mL of this tracer-containing seawater was percolated through the syringe core. This addition was equivalent to 200 kBq $^{35}SO_4^{2-}$ per sample. Sediments were incubated at room temperature in the dark for 6 h. To stop the reaction, sediment samples were transferred to 6 mL 20% (w/v) ZnAc and stored at −20°C. The pool of reduced ^{35}S was separated from the pool of unreacted ^{35}S ($^{35}SO_4^{2-}$) by cold acidic Cr^{2+} distillation (Røy et al. 2014). Radioactivity was determined by scintillation counting (Perkin-Elmer Tri-Carb 4910 TR; Ultima-Gold Scintillation cocktail) and SRR were calculated as described previously (Røy et al. 2014).

SO_4^{2-} reduction rates in experiments

In order to assess the influence of kelp deposition on SRR, SRR were determined in syringe cores with either only kelp, sediment-only from the kelp-beach, or kelp plus sediment from the kelp-beach, each in four replicates. In the experiments, either 0.5 g of kelp, 3 mL of sediment, or 0.5 g of kelp plus 3 mL of sediment was used. Sediments comprised a mixture of the top 10 cm of kelp-beach sediments. To mimic beach conditions, the sediments were exposed to air at 4°C until use 2 d later. Intact *Laminaria hyperborea* plants were sampled from fresh kelp deposits on the kelp-beach in parallel to the sediment sampling, and stored at 4°C until use 2 d later. The kelp fragments were cut from the middle of *Laminaria hyperborea* leaves. Kelp fragments were mixed with the sediments. The samples were incubated and SRR were determined as described above.

Microbial community composition

Collection of water, sediment, and white filaments

Water was collected from the beaches, harbors and promenades around the main island of Helgoland with a bucket and filtered on 0.22 μm pore-size polyethersulfone filters (47 mm diameter, Millipore). The filters were frozen at −20°C and stored until further analysis. Sediment cores were collected at the kelp-beach and reference beach. At the kelp-beach, cores were taken from the sediment at the low tide waterline and from sediment below a kelp deposit. From each layer 0.4 g of sediment was frozen at −20°C for DNA extraction. At the low tide waterline of the kelp-beach, pieces of green algae completely covered with white filaments were collected in 15 mL tubes and stored at −20°C until further processing.

DNA extraction

DNA was extracted from a quarter of a polyethersulfone filter, corresponding to ca. 0.4 g of sediment or ca. 0.1 g of white filaments, using the MoBio PowerSoil DNA extraction kit (MoBio, Carlsbad) with an additional Proteinase K digestion and heating at 65°C step as described previously (Meier et al. 2017).

16S rRNA amplification, sequencing, and analysis

For a detailed description of the 16S rRNA amplification, sequencing, and analysis, see Supplementary Materials and Methods.

Metagenome sequencing and analysis

For a detailed description of the sequencing, assembly, binning, and annotation, see Supplementary Materials and Methods.

Fluorescence in situ hybridization

Frozen white filaments were thawed on ice and immediately fixed with 1.5% formaldehyde in 1× PBS (pH = 7.4) at 4°C overnight. Fixed material was filtered on a 0.22 μm polycarbonate filter (Millipore). The filter was excessively flushed with 1× PBS to remove the remaining formaldehyde. For fluorescence in situ hybridization (FISH), filter slices were incubated with fluorescently double-labeled oligonucleotide probes in a 35% formamide containing hybridization buffer for 3 h at 46°C. The GAM42a probe (Manz et al. 1992) labeled with two Atto-488 fluorochromes was used to detect *Gammaproteobacteria* cells, and a mix of SFO1112 and SFO1210 probes (McNichol et al., https://osf.io/yts4p/, accessed on 18 July 2020) labeled with two Atto-594 fluorochromes to detect *Sulfurovum* cells. Visualization was done on an Axioplan epifluorescence microscope (Zeiss).

Total cell counts

Sampling was conducted at 6 locations on the kelp-beach (3 locations below kelp deposits, 3 locations next to kelp deposits), and 2 locations on the reference beach. Samples were obtained from 0 to 2, 2 to 4, 5 to 7, and 9 to 11 cm depth. A volume of 0.5 mL of sediment was fixed using 1 mL of 2% formaldehyde for 1–1.5 h at room temperature. Samples were then centrifuged, the supernatant removed, and replaced by 1 mL 1:1 ethanol:1× PBS. Samples were again centrifuged, the supernatant removed, and 1 mL 1:1 ethanol:1× PBS added. The samples were stored at −20°C until further use. Ultrasonication was used to remove cells from the sediment (3× 30 s at 20% power). After each round, 1 mL of supernatant was removed and replaced by 1 mL 1:1 ethanol:1× PBS. Supernatant was stored at −20°C. A volume of 50 μL of supernatant was filtered on polycarbonate membrane filters (pore size of 0.2 μm). Cells on the filter were stained with DAPI. Cell counting was conducted under an epifluorescence microscope.

Nucleotide sequence accession numbers

All sequence data have been deposited in the European Nucleotide Archive under project number PRJEB36085.

Results

Description of the sampling sites

The kelp-beach and reference beach consisted of predominantly sandy sediments, mixed with gravel and stones. Sediments from the kelp-beach occasionally had a dark-gray appearance. The porosity was 0.28 ± 0.08 for kelp-beach and 0.26 ± 0.08 for reference beach sediments, respectively. The unexpectedly low porosity for sands could be due to the presence of small air bubbles in the sediments. The average TOC content in kelp-beach sediments is slightly higher than in reference beach sediments ($0.04\% \pm 0.02\%$ ($n = 24$) vs. $0.02\% \pm 0.01\%$ ($n = 19$), equal to 61.9 g C m^{-2} vs. 26.2 g C m^{-2} after integration over the sample depth of 0–10 cm). Both values are remarkably low and not statistically different.

Kelp deposits occurred on the kelp-beach during all field campaigns; however, the amount of material in the deposits was variable in time and space (Fig. 2a,b). In November 2017,

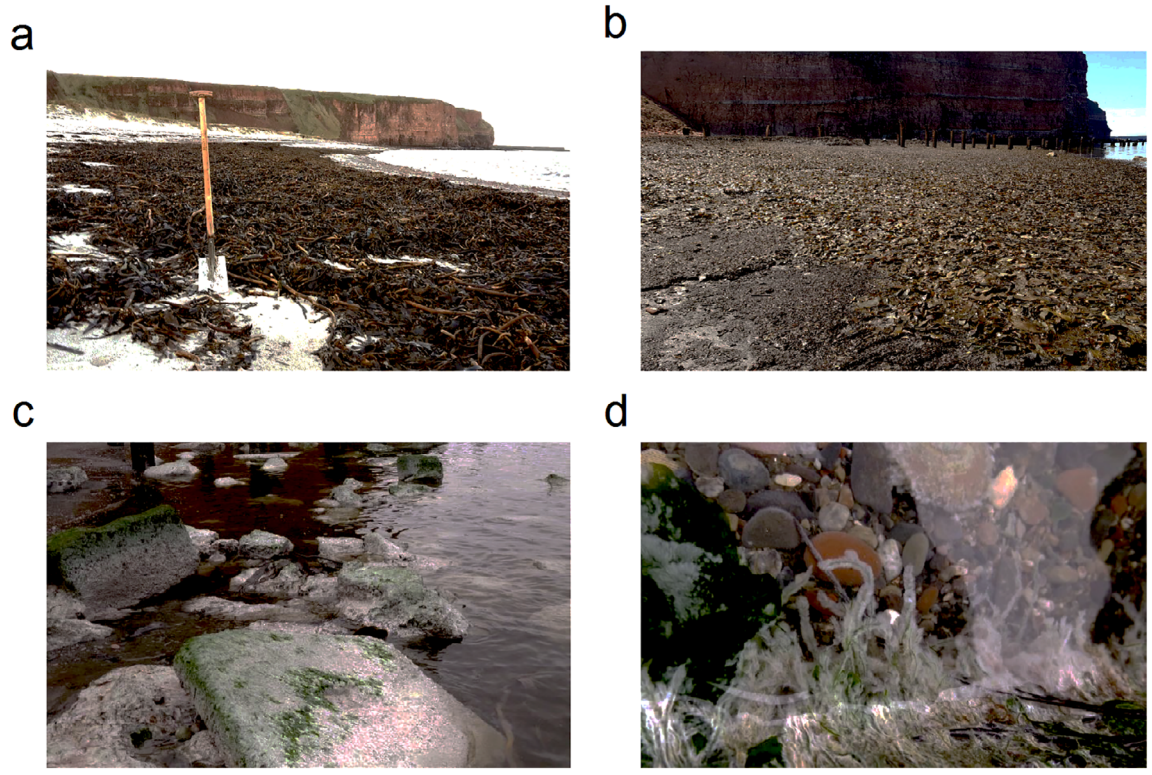

Fig. 2. The kelp-beach with dominantly *Laminaria* deposits in November 2017 (**a**) and May 2018 (**b**). White filaments covering green algae on rocks at the low tide waterline of the kelp-beach in October 2015, in overview (**c**) and in close-up (**d**).

October 2018, July 2019, and August 2019, kelp deposits were patchy and mainly occurred close to the edges of the beach, while relatively small amounts were present at the center of the beach. In October 2015 and May 2018, kelp covered the whole beach, with 15 m wide, 0.5 m thick deposits. Kelp was partially fragmented to pieces of down to lengths of centimeters to several decimeters. The deposits were usually inhabited by kelp flies and the beach was occasionally pervaded by an intense sulfidic smell. Kelp fragments were buried down to at least 30 cm in the sediment. The investigated deposits were inundated during high tide and exposed during low tide. In October 2015, green algae on rocks at the low tide waterline of the sea adjacent to the kelp-beach were completely covered with a bloom of white filaments (Fig. 2c,d). Close to the low tide waterline, the outflowing porewater was milky and had a strong sulfidic smell. During this field campaign, the weather was very calm with nearly no wind and waves. On the reference beach, kelp deposits were absent during all field campaigns.

In situ geochemical analyses

Concentrations of degradation products of organic material were elevated within sediments from the kelp-beach, but were highly variable and within the depth layer investigated, no trend could be observed. In November 2017, DOC was elevated by approximately 5 mmol L^{-1} and DIC by 10 mmol L^{-1} in October 2018 (Fig. 3a,b). In May 2018, SO_4^{2-} concentrations were ~15 mmol L^{-1} lower in kelp-beach sediments compared to reference beach sediments (Fig. 3c), and depleted in equal extent compared to seawater (average kelp-beach seawater SO_4^{2-} concentration is 23.2 ± 2.3 mmol L^{-1}, that of reference beach seawater is 26.3 ± 0.3 mmol L^{-1}). These lower concentrations are not due to dilution with freshwater, since porewater Cl^- concentrations were similar to those of seawater. Indeed, sulfide levels were strongly elevated relative to reference beach porewater levels (by about 10 mmol L^{-1}) (Fig. 3d), indicating conversion of SO_4^{2-} to sulfide. The levels of DIC, SO_4^{2-}, and sulfide correspond roughly with the stoichiometry of SO_4^{2-} reduction by the oxidation of organic material:

$$2CH_2O + SO_4^{2-} \rightarrow H_2S + 2HCO_3^-,$$

where per mol of reduced SO_4^{2-} 1 mol of sulfide and two moles of DIC are produced. In sediments from the reference beach, no sulfide was detected (Fig. 3d). Sulfide was present in 9 out of 13 seawater samples from seawater adjacent to the kelp-beach in May 2018, taken at times when microsensor measurements were made, in concentrations between 0.05 and 4.27 mmol L^{-1}.

Fe(II) was the dominant form of solid-phase Fe in kelp-beach sediments. Conversely, Fe(III) was the main form of solid-phase Fe in reference beach sediments (Table 2). In sediments from the kelp-beach, solid-phase, Fe(III) was thus

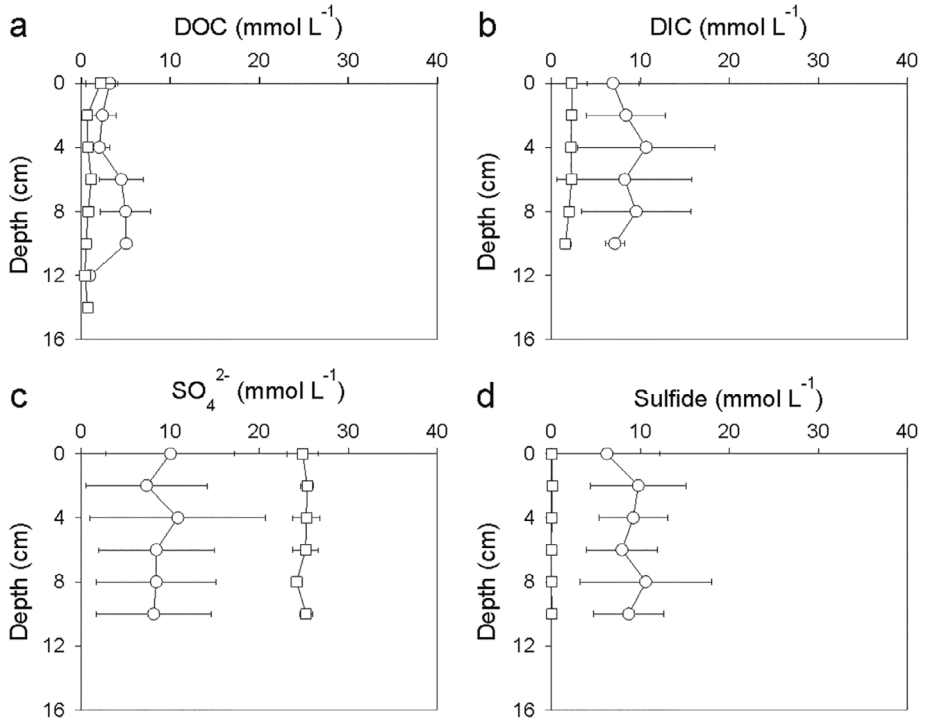

Fig. 3. Dissolved organic carbon (DOC; **a**), dissolved inorganic carbon (DIC; **b**), SO_4^{2-} (**c**) and sulfide (**d**) within porewaters from the kelp-beach (○) and the reference beach (□).

quantitatively reduced to Fe(II), while in the reference beach sediments net Fe(III) reduction did not occur, at least was much slower than Fe(II) oxidation. Dissolved Fe was negligible, compared to the concentrations of solid-phase Fe (Table 2).

Concentrations of the nutrients NH_4^+ and P_i were elevated in porewater of kelp-beach sediments, likely due to kelp biomass degradation. P_i could furthermore have been released by minerals during their reduction. On the other hand, $NO_3^- + NO_2^-$ concentrations were reduced (Fig. 4), probably due to denitrification driven by kelp degradation. These features were mainly occurring during periods with relatively high amounts of deposited kelp (May 2018), and were less pronounced in November 2017, when kelp deposits were not that extensive. Denitrification was furthermore indicated by higher N_2O concentrations in kelp-beach sediments (Table 2). Sediments from the kelp-beach also had slightly elevated CH_4 concentrations, indicating methanogenesis (Table 2). Nutrient and DOC concentrations were occasionally high in seawater adjacent to the kelp-beach (data not shown), with maximum concentrations of 2400, 30, 85, and 1300 μmol L^{-1} for NH_4^+, $NO_3^- + NO_2^-$, P_i, and DOC, respectively. These concentrations are 1 to 2 orders of magnitude higher than average concentrations in seawater adjacent to the reference beach for NH_4^+, $NO_3^- + NO_2^-$, and P_i (May 2018), and 5 times higher for DOC.

Table 2. Solid-phase Fe (Fe(II) and Fe(III)) and dissolved Fe (Fe^{2+}), N_2O, CH_4, CO and H_2 concentrations for sediments from the kelp-beach and sediments from the reference beach. Values are averages over separate profiles, since no trend with depth or location on the beaches was evident.

	November 2017		May 2018		October 2018	
	Kelp-beach	**Reference beach**	**Kelp-beach**	**Reference beach**	**Kelp-beach**	**Reference beach**
Fe(III) (mmol L^{-1} sed)					17.44 ± 56.40	9.25 ± 1.95
Fe(II) (mmol L^{-1} sed)					127.02 ± 128.81	0.62 ± 0.19
Fe^{2+} (μmol L^{-1} sed)					4.47 ± 4.05	0.86 ± 0.08
N_2O (μmol L^{-1} sed)			0.46 ± 0.39	0.13 ± 0.19		
CH_4 (μmol L^{-1} sed)			4.69 ± 4.36	1.58 ± 1.53		
CO (μmol L^{-1} sed)	0.18 ± 0.15	0.09 ± 0.07	1.34 ± 0.99	0.51 ± 0.50		
H_2 (μmol L^{-1} sed)	0.79 ± 0.52	0.53 ± 0.13	0.50 ± 0.22	0.33 ± 0.06		

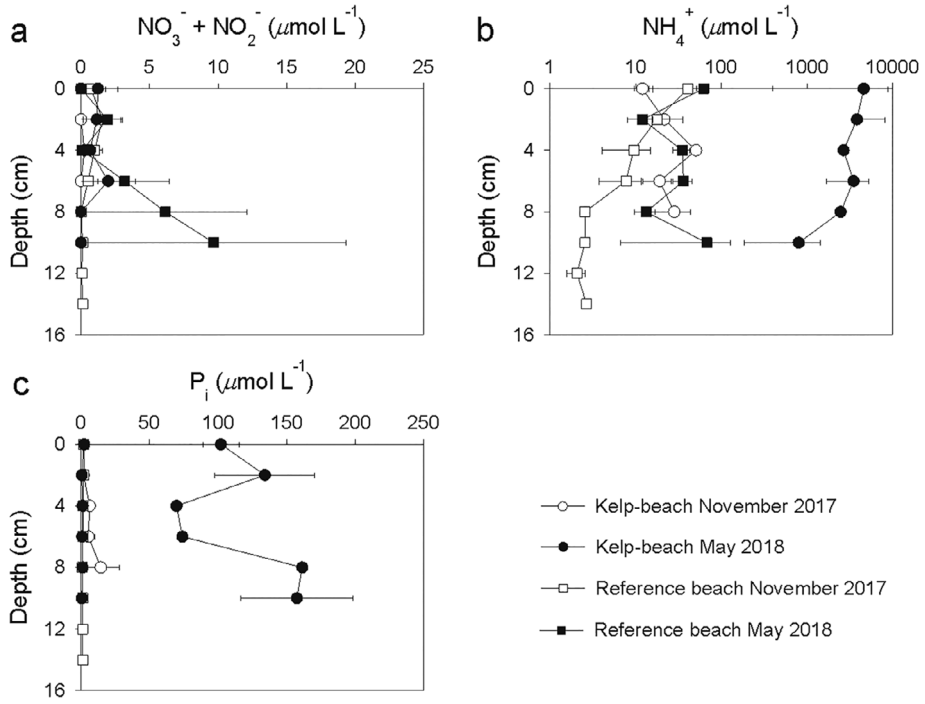

Fig. 4. Porewater NO_3^- + NO_2^- (**a**), NH_4^+ (**b**), and inorganic phosphorus (Pi; **c**) concentrations from sediments of the kelp-beach in November 2017 (○) and May 2018 (●) and from sediments of the reference beach in November 2017 (□) and May 2018 (■).

In situ microsensor measurements in kelp-beach sediments show highly dynamic O_2 and pH profiles in response to the tides (Fig. 5). During low tide, O_2 is depleted within sediments from the kelp-beach (both below and next to the kelp deposits). Conversely, during high tide, O_2 quickly penetrates the surface sediments by hydraulic forcing. Thus, high diffusive O_2 fluxes exist in sediments covered by, or next to, kelp deposits (4.2×10^{-8} and 2.1×10^{-8} mol m^{-2} s^{-1}). The volumetric O_2 consumption rate was 3.3×10^{-4} mol m^{-3} s^{-1}, which would result in an areal O_2 consumption rate of 2.7×10^{-6} mol m^{-2} s^{-1}. During low tide, O_2 did not penetrate the sediments and O_2 consumption had thus stopped. The pH values during low tide were low, reaching minima of around 6.7. Seawater coverage quickly elevated the pH in the upper 2.5 cm, indicating rapid water exchange. The top 3.5 cm of reference beach sediments stayed oxic at low tide, and the pH values remained close to those in seawater (7.9). The diffusive O_2 flux in reference beach sediments was 2.7×10^{-10} mol m^{-2} s^{-1}, which was 2 orders of magnitude lower than the diffusive O_2 fluxes in kelp-beach sediments. The volumetric O_2 consumption rate was 3.6×10^{-5} mol m^{-3} s^{-1}, which is one order of magnitude lower than for kelp-beach sediments. This would result in an areal O_2 consumption rate of 1.3×10^{-6} mol m^{-2} s^{-1}, which is 2 times lower than in kelp-beach sediments.

The porewater $S^{2-}{}_{tot}$ concentrations are extremely high within surface sediments from the kelp-beach, reaching maxima of more than 15 mmol L^{-1} during low tide (Fig. 5). These levels are comparable to dissolved total sulfide levels measured by porewater extraction (Fig. 3d). It should be noted that calculations of $S^{2-}{}_{tot}$ from pH and H_2S profiles are inaccurate in dynamic conditions, because the alignment of pH and H_2S profiles is uncertain. The $S^{2-}{}_{tot}$ concentrations are below detection limit within sediments from the reference beach. No H_2S was detected in reference beach sediments. The low pH, high diffusive O_2 fluxes and O_2 consumption rates, and high $S^{2-}{}_{tot}$ levels in kelp-beach sediments indicate high rates of fermentation, aerobic respiration, and SO_4^{2-} reduction.

Both CO and H_2 concentrations were elevated within sediments from the kelp-beach compared to sediments from the reference beach (Table 2). The CO concentrations were highest in May 2018, whereas H_2 concentrations were highest in November 2017.

CO and H_2 evolution in laboratory experiments

Net CO and H_2 formation only occurred in incubations with kelp, and their concentrations were inversely correlated to O_2 concentrations (Fig. 6). When O_2 was present in the headspace, CO was quickly produced. After around 200 h of incubation, when O_2 concentrations were as low as 12 μmol L^{-1}, net production ceased. The CO concentration at that time was 37 μmol L^{-1}. Importantly, no further change in CO concentration was observed during the anoxic phase. Net H_2 production, on the other hand, mainly occurred at low O_2 concentrations. The majority of H_2 production occurred after 72 h, when O_2 concentrations were below 26 μmol L^{-1}. Both CO and H_2 could thus be produced from degrading kelp. Net

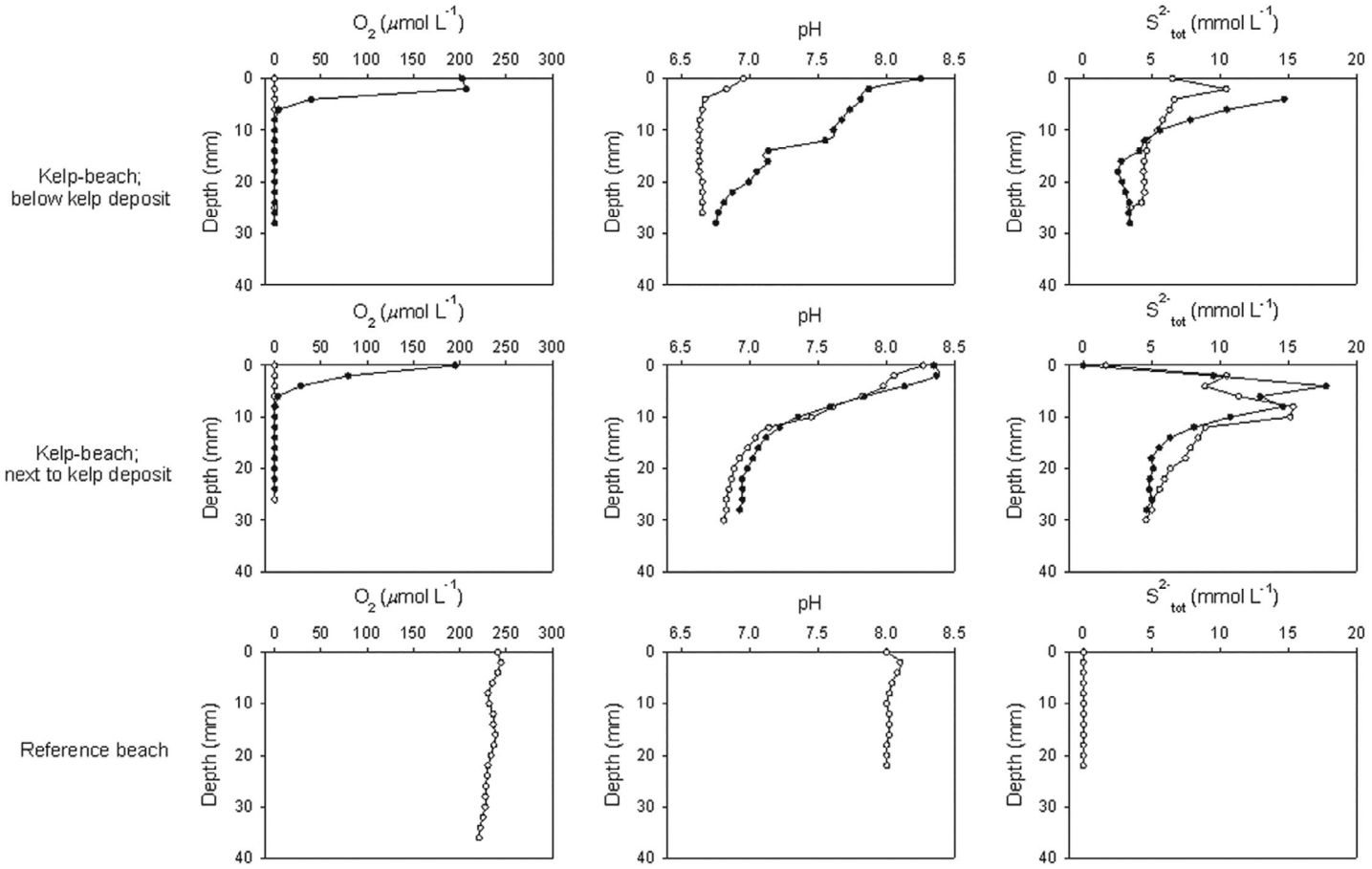

Fig. 5. O_2 (left panels), pH (middle panels) and total sulfide (S^{2-}_{tot}; right panels) microprofiles within kelp-beach sediments (top and middle panels) and within reference beach sediments (bottom panels) during low tide (o) and incoming tide (●). The top panels show profiles within sediments below kelp deposits and the middle panels profiles within sediments next to kelp deposits. Incoming tide profiles refer to the moment when seawater starts to cover the site, while during low tide, the sites are exposed.

CO production mainly occurs under high O_2 conditions, while low O_2 conditions are needed for significant H_2 accumulation. No significant net production of either CO or H_2 took place within the kelp-free controls.

Calculated production rates within artificial seawater were converted to production rates within sediment using the porosity of kelp-beach sediment. Sedimentary net production of CO occurred with a rate of $1.22\times 10^{-7} \pm 0.24\times 10^{-7}$ mol m^{-3} s^{-1} during the first 6 h of incubation. Net H_2 production rates were determined during the period of fastest increase (120–264 h). During this period, sedimentary net H_2 production was $1.13\times 10^{-8} \pm 0.27\times 10^{-8}$ mol m^{-3} s^{-1}.

SO_4^{2-} reduction rates

The SRR was extremely variable in the kelp-beach sediments, as reflected in the large standard deviation (Table 3). The lack of a clear trend with depth or location (below deposits vs. next to deposits) reflected a heterogeneous distribution of kelp fragments. Rates varied with 2 orders of magnitude within individual depth profiles and between depth

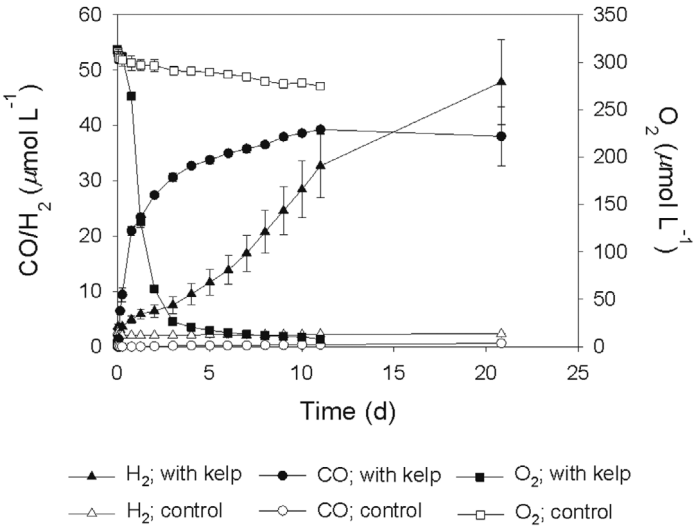

Fig. 6. H_2 (triangles), CO (circles) and O_2 (squares) concentrations within incubations with kelp (filled symbols) and within controls (open symbols).

profiles (Table 3). All rates for sediments from the reference beach were below the minimum detection limit of 2.46×10^{-9} mol m^{-3} s^{-1} (Table 3).

The average SRR in sediments from the kelp-beach was $3.77\times 10^{-6} \pm 6.34\times 10^{-6}$ mol m^{-3} s^{-1} (Table 3; median was 1.25×10^{-6} mol m^{-3} s^{-1}). The SO_4^{2-} turnover time was 13 d, as calculated by dividing the depletion of SO_4^{2-} per volume sediment (15 mol depletion m^{-3} porewater× porosity of 0.28 = 4.2 mol depletion m^{-3} sediment) by the average SRR of 3.77×10^{-6} mol m^{-3} s^{-1}.

Addition of kelp leaf fragments to kelp-beach sediments led to a 20- to 25-fold increase in SRR. In treatments with only kelp, no SO_4^{2-} reduction occurred (average counts over the 4 treatments is below the minimum detection limit), and in treatments with only sediment SRR are low (average $0.31\times 10^{-6} \pm 0.12\times 10^{-6}$ mol m^{-3} s^{-1}; median 0.26×10^{-6} mol m^{-3} s^{-1}). Only the mixture of kelp leaf fragments and sediment leads to a direct stimulation of SRR, resulting in an average rate of $7.06\times 10^{-6} \pm 2.49\times 10^{-6}$ mol m^{-3} s^{-1} (median of 8.12×10^{-6} mol m^{-3} s^{-1}). The SO_4^{2-} turnover time calculated using the average SRR from this experiment (7.06×10^{-6} mol m^{-3} s^{-1}) and the 4.2 mol depletion m^{-3} sediment is 7 d.

Microbial community composition

In order to assess the effect of kelp deposition on the microbial community composition, we performed 16S rRNA gene amplicon sequencing of the DNA extracted from different sediment layers from the kelp-beach and the reference beach. Additionally, we sequenced the white filaments growing on green algae on rocks at the kelp-beach low tide waterline and samples of seawater from the beaches and harbors around the main island of Helgoland. An overview of the sequencing efforts can be found in Supplementary Information (Table S1).

We clustered the samples based on the similarity of their microbial community composition on SWARM-generated OTU level (Fig. 7). All samples clustered based on the sample type and location they were coming from.

In general, the community in kelp-beach sediment differed from that in reference beach sediment by showing higher average proportions of the fermenters, such as *Clostridia* (4% compared to 0.3%), *Fusobacteria* (3.4% compared to 0.8%), *Kiritimatiellaeota* (4.2% compared to 0.2%), *Gracilibacteria* (2.3% compared to 0.05%), *Spirochaetes* (3% compared to 0.3%), the SO_4^{2-} reducing *Deltaproteobacteria* (13% compared to 8%), and the sulfide-oxidizing *Epsilonbacteraeota* (17% compared to 3%) (Fig. 7). In the three deepest layers of kelp-beach sediments, the methanogenic archaea *Methanolobus* was present, albeit in very low proportion (0.02–0.04%).

For samples next to kelp deposits, a clear shift of the microbial community composition with depth was apparent (Fig. 7). With depth *Epsilonbacteraeota* (consisting of *Sulfurovum* and *Sulfurimonas*) dramatically decreased (from 40% to 4.5%), while *Deltaproteobacteria*, *Bacteroidetes*, *Clostridia*, *Fusobacteria*, *Kiritimatiellaeota*, and *Spirochaetes* increased (all together from 23% to 49%; Fig. 7).

No trend with depth and only little variation in microbial community was detectable in samples from below kelp deposits. The proportion of *Desulfobacteraceae* (*Deltaproteobacteria*) sequences was constant with depth (12% ± 2%). Proportions of *Clostridia*, *Kiritimatiellaeota*, *Gracilibacteria*, and *Spirochaetes* were higher than in reference beach samples but lower than in the kelp-beach sediment from next to a deposit. The sediment samples taken below a kelp deposit also had increased proportions of *Thiotrichaceae* sequences (10%) and the highest proportions of *Bacteroidetes* (24%).

The community of the white filaments had a higher similarity to that of sediment samples from below kelp deposits than to the communities of reference sediment and seawater (Fig. 7). The communities of the white filaments were dominated by *Thiotrichaceae* (on average 32%) and *Sulfurovum* (on average 39%) sequences, with only small proportions of *Bacteroidetes* (on average 4%), *Gracilibacteria* (on average 4.8%), and *Alphaproteobacteria* (on average 4%). The *Thiotrichaceae* and *Sulfurovum* sequences were also found in all other samples, but in lower relative abundances (not higher than 7.5% and 21%, respectively). *Sulfurimonas* sequences which were co-occurring with *Sulfurovum* in all other samples (Fig. 7) were absent from the samples of the white filaments. Interestingly, the two OTUs constituting the large part of *Sulfurovum* sequences in the white filaments (on average 27%) and the sediment under the kelp deposit (on average 5.8%) were only found in very low relative abundance in all other samples (not higher than 3.8%). The most abundant *Sulfurovum* OTU in the sediment samples from next to a kelp

Table 3. SO_4^{2-} reduction rate (SRR) for sediments from the kelp-beach and the reference beach and from the kelp deposition simulation experiment with sediment from the kelp-beach. Also shown are the minimum and maximum rates for kelp-beach sediments. SRR within reference beach sediments was below the minimum detection limit (2.46×10^{-9} mol m^{-3} s^{-1}).

	Average SRR (mol m^{-3} s^{-1})	Maximum SRR (mol m^{-3} s^{-1})	Minimum SRR (mol m^{-3} s^{-1})
Kelp-beach	$3.77 \times 10^{-6} \pm 6.34 \times 10^{-6}$	2.23×10^{-5}	2.05×10^{-7}
Reference beach	Below minimum detection limit	—	—
Experiment			
Sediment	$0.31 \times 10^{-6} \pm 0.12 \times 10^{-6}$		
Kelp plus sediment	$7.06 \times 10^{-6} \pm 2.49 \times 10^{-6}$		

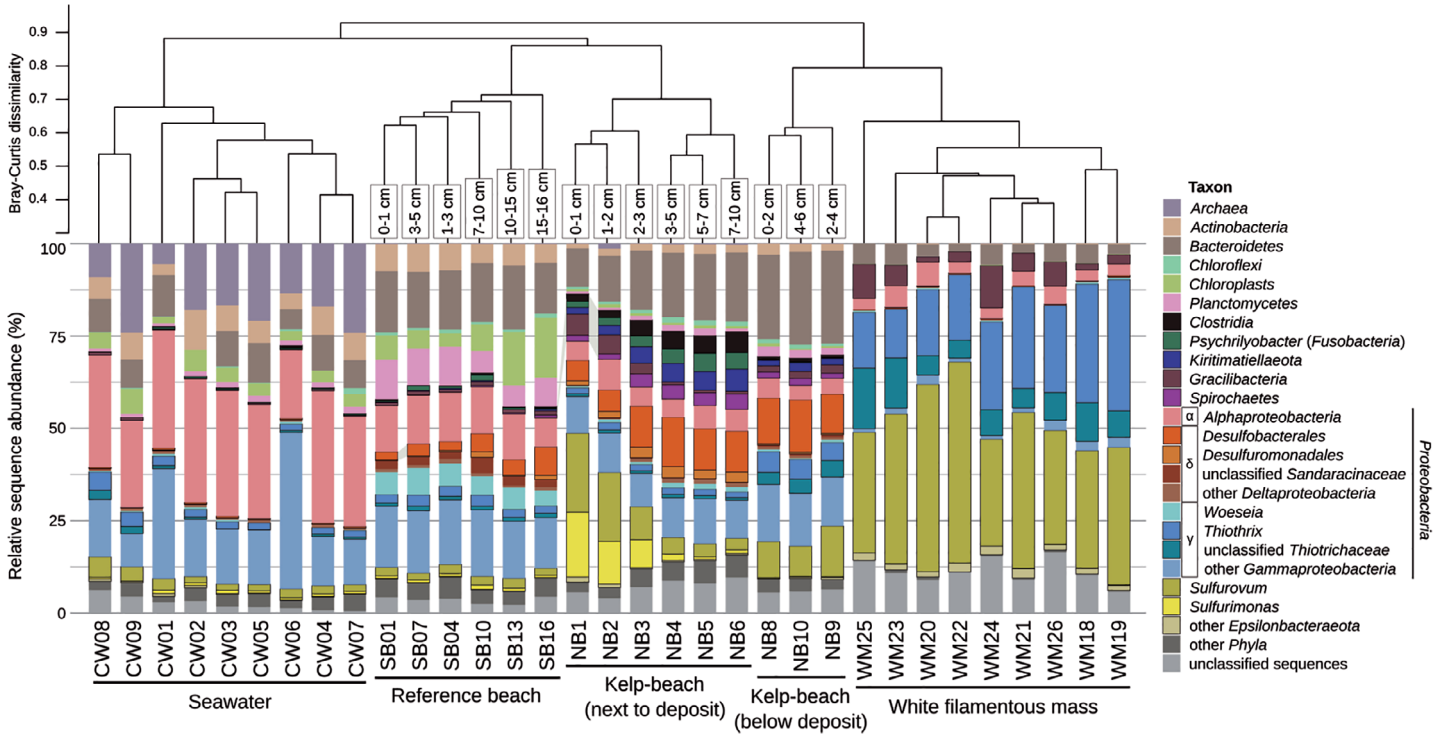

Fig. 7. Microbial community composition based on 16S rRNA gene amplicon sequences. Samples were clustered based on their community composition according to a Bray–Curtis dissimilarity matrix. For the sediment samples the depth in cm is indicated above the bars.

deposit and in the reference beach samples did not surpass 0.6% in the sediment under the kelp and white filaments.

Detection of *Sulfurovum* by FISH

We performed FISH with a *Gammaproteobacteria*-specific probe (GAM42a) and *Sulfurovum*-specific probe mix (SFO1112 and SFO1210, McNichol et al., https://osf.io/yts4p/, accessed on 18 July 2020). We could detect both groups growing as filaments directly next to each other, attached to green algae on rocks at the low tide waterline (Fig. 8), thus within the oxic seawater environment.

Genomic potential of filamentous biomass

We sequenced three metagenomes of the white filaments and performed metagenomic binning to obtain population genomes (bin metrics in Supplementary Information, Table S1). Our assembly is representing over 69% of the raw reads based on read mapping. Over 84% of the assembled metagenome is in bins with over 50% completeness and less than 10% contamination (based on CheckM analysis).

We obtained a total of six *Sulfurovaceae* (according to GTDB classification) population genomes (81–99% completeness, 1–5% contamination) and compared their genomic potential to other published *Sulfurovum* genomes and metagenomic bins (Fig. 9). The potential for oxidizing reduced sulfur species (sulfide: quinone reductase and SOX system encoding genes) as well as the potential for CO_2-fixation via reductive tricarboxylic acid cycle was present in all genomes. The difference with published *Sulfurovum* genomes with respect to the basic energy generation metabolism seemed to occur on the electron acceptor side. Our genomes lack the genes for NO-forming nitrite reductase and nitric- and nitrous-oxide reductases. Thus, these aerobic sulfur oxidizers cannot perform denitrification.

Another difference was the presence of a low-affinity Cytochrome C oxidase (aa3, Type A2), which was not found in most of the other genomes, except *Sulfurovum* sp. isolated from marine sediment, *Sulfurovum* genome from a surface biofilm in the Frassassi caves, a mine drainage run-off metagenomic bin and in one of the hydrothermal genomes. However, all *Sulfurovum* genomes also encoded genes for the high-affinity Type-C (cbb3) terminal oxidase.

Another gene unique to the Helgoland bins was encoding a Ferritin-like antioxidant protein hinting at an increased ability of tolerating exposure to O_2.

Total cell counts

The amount of cells on the kelp-beach was not much higher than on the reference beach ($2.18\times 10^8 \pm 5.33\times 10^7$ cells cm^{-3} sediment compared to $1.82\times 10^8 \pm 2.63\times 10^7$ cells cm^{-3} sediment). Considering the big difference in rates of microbially mediated processes, this small difference in cell numbers suggests that the microbial community at the kelp-beach is more active.

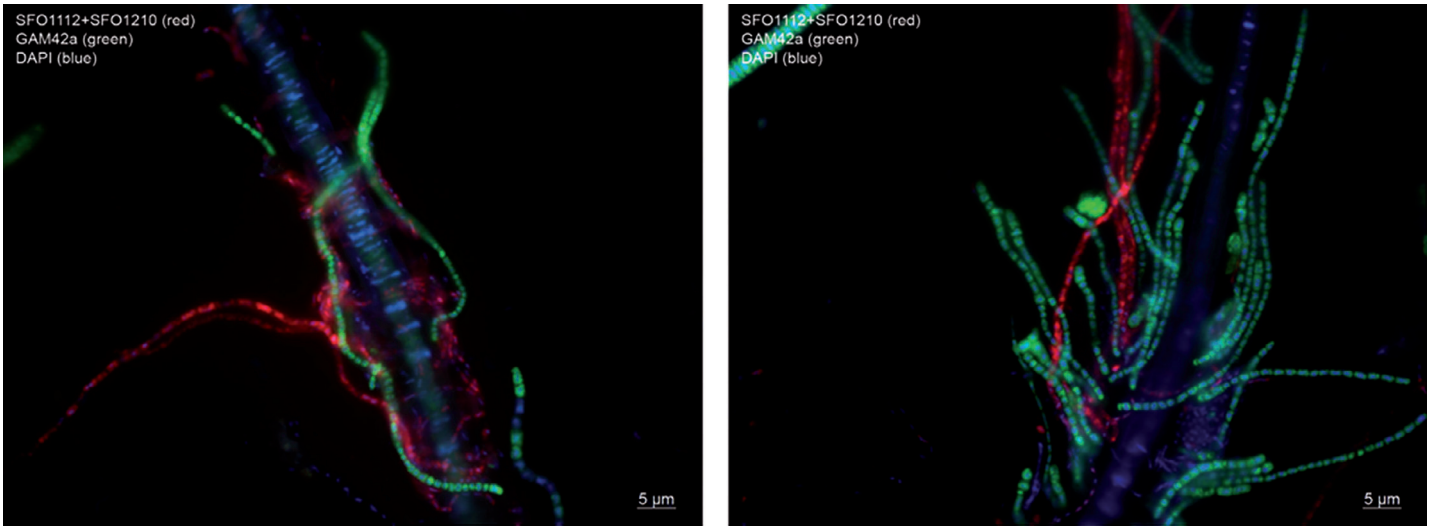

Fig. 8. Fluorescent microscopy images of sulfur-oxidizing bacterial filaments attached to the green algae. The cells are labeled with *Gammaproteobacteria*- (GAM42a; in green), and *Sulfurovum*-specific (SFO1112 + SFO1210; in red) rRNA probes. DAPI signals are shown in blue.

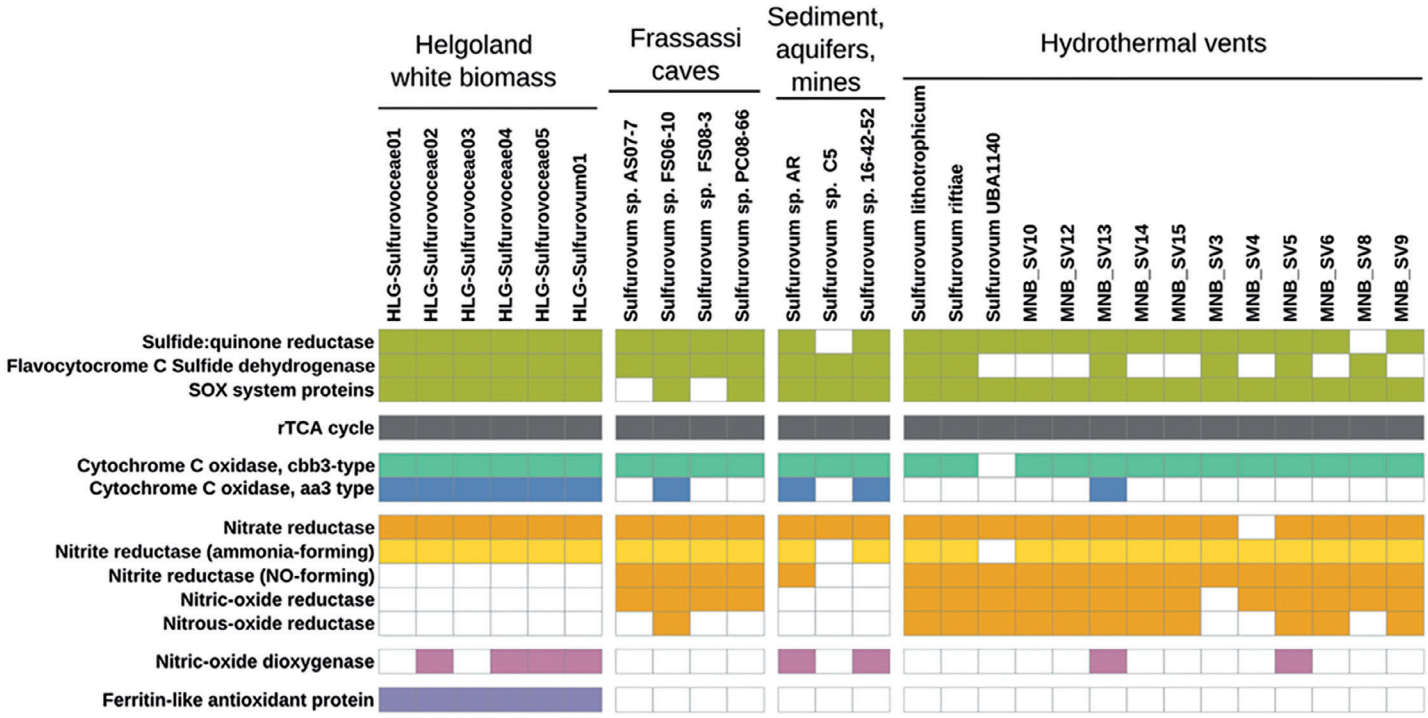

Fig. 9. Basic genomic potential of the *Sulfurovum*-related bins in comparison to other sequenced *Sulfurovum* genomes and metagenomic bins (Meier et al. 2017), with project accession number PRJEB15554. The comparison was mainly based on presence-absence of orthologous clusters based on EggNOG annotation and cross-checked with the other annotation sources: BLAST vs. (point behind the s) Uniprot, RAST, Pfam. For the *Sulfurovum* UBA1140 genome genes were predicted and annotated de-novo. All annotations can be found in Supplementary Information (Table S3).

Discussion

Kelp deposits that are not swept back out to sea by the next tide become partly buried, decomposed, and eventually heterogeneously distributed as fragments over the beach surface and within the sediment. Burial of kelp fragments thus leads to mixing of fresh and decayed organic material. Kelp fragments are composed of both labile and refractory compounds, which are degraded at different rates. Intertidal zones are dynamic systems, in which changes in hydration, temperature and salinity can be large and fast. All these factors will lead to

a high variability in decomposition rates. Laboratory measured rates must therefore be seen as approximates of rates occurring in situ.

Kelp deposition is the main factor in shaping the composition and function of the microbial communities at the kelp-beach and the main cause of the observed differences between the two studied beaches. The sediment characteristics were nearly identical (Supplementary Information, Table S2), and can thus not be the main determinant for the different geochemistries. The dominant winds around Helgoland are west-southwesterly (Siegismund and Schrum 2001), and the residual currents are north–south oriented (von Haugwitz et al. 1988). The kelp-beach faces northwest and the reference beach southeast. The kelp-beach is adjacent to rocky seafloor covered with kelp forests (Uhl et al. 2016). The reference beach does not face a large kelp forest (Uhl et al. 2016) and wind and current directions are not oriented toward the beach. Therefore, the kelp-beach is regularly covered with kelp, while the reference beach is not, thus kelp deposits are the main determinant for the distinct geochemistry of the kelp-beach.

Although the heterogeneity of the sediments was reflected in the geochemical data that showed very large standard deviations and scattered trends with depth, our data demonstrated that the presence of kelp deposits strongly enhanced microbial degradation processes. Furthermore, the release of reduced material was so large that it cannot be oxidized locally, driving a sulfuretum in the adjacent sea. Such phenomena are restricted to beaches near rocky coasts, as kelp needs a hard substrate to attach. This study extends the knowledge on mineralization pathways of kelp deposited on beaches, as it combines both geochemical and microbial community data, and shows that kelp deposition leads to unique conditions. Especially, the high SO_4^{2-} reduction can induce high concentrations of free sulfide, even in the oxic parts of the ecosystem. This in turn leads to a distinct microbial community within sediments and on solid surfaces in the adjacent sea. Fragmentation by physical forces and macro- and meiofauna will facilitate and stimulate the subsequent microbial processes, of which hydrolysis, fermentation, aerobic respiration, Fe reduction, and SO_4^{2-} reduction will be discussed sequentially.

Hydrolysis and fermentation processes

Elevated DOC levels plus the strongly enhanced consumption of electron acceptors indicated that hydrolysis was active and extremely fast. Active fermentation was demonstrated by the low pH, much lower than can be explained by CO_2 production during aerobic respiration alone. CO_2calc is a program for calculations on the DIC system, which relates a suite of relevant input parameters to determine the concentration and speciation of the DIC system. CO_2calc v. 2.1.0 (Robbins et al. 2010) was used to assess the change in pH as a result of CO_2 production by aerobic respiration. First, the total CO_2 concentration in the kelp-beach porewaters was calculated to be 2.23 mmol kg^{-1}. Subsequently, the pH was calculated for a situation in which all O_2 is consumed and thus an equal amount of CO_2 is released. This total removal of O_2 and thus increase in CO_2 equals 0.21 mmol kg^{-1}, leading to a new total CO_2 concentration of 2.44 mmol kg^{-1}. Input of this new total CO_2 concentration resulted in a pH value of 7.58, which is thus the value that is induced by aerobic respiration. As porewater may be more strongly buffered than seawater, the actual decrease by respiration may even be overestimated. SO_4^{2-} reduction will not lead to a further decrease (Soetaert et al. 2007). Furthermore, sulfide oxidation will not be of importance, as the sediments are anoxic. Hence, the only process that can drive the pH down to 6.7 is the production of organic acids by fermentation.

Elevated hydrolysis and fermentation within kelp-beach sediments is furthermore supported by the higher abundances of polymer hydrolysers like *Bacteroidetes* and fermenters like various *Clostridiales*, *Psychrilyobacter*, *Kiritimatiellaeota*, and *Spirochaetes* (see https://lpsn.dsmz.de, accessed on 18 July 2020) in kelp-beach sediments.

SO_4^{2-} reducing bacteria cannot use complex and large organic molecules, and these kelp-derived molecules must thus first be hydrolysed and fermented to e.g., volatile fatty acids and H_2. Fermentation is therefore an important intermediate process in this environment, as SO_4^{2-} reduction occurs extensively.

The pathway of electron transport from fermentation to SO_4^{2-} reduction via DOC was considered to be significant, since fermentation occurred intensively, and DOC concentrations in porewaters were high (up to 8.9 mmol L^{-1}).

Aerobic respiration

It appeared to be difficult to determine aerobic respiration reliably, as the transport mechanisms could not well be constrained. The O_2 fluxes determined from the profiles assuming diffusion as transport process underestimated the aerobic respiration, as also advective transport will occur. Conversely, the areal O_2 consumption rates determined from the volumetric rates and the penetration depth overestimated the aerobic respiration, as the sediments were homogenized and sieved, hence also strongly reduced deeper sediments, that normally would not be in contact with O_2 were taken into the calculation. Furthermore, in situ, the kelp deposits could physically restrict advective transport of seawater and thereby O_2 into the sediments, leading to a lower penetration depth. O_2 only penetrated the kelp-beach sediments during inundation. Thus, the rates were corrected for the inundation time of 16 h d^{-1}. The diffusive O_2 flux was 2.8×10^{-8} mol m^{-2} s^{-1} (below a kelp deposit) and the areal O_2 consumption rate was 1.8×10^{-6} mol m^{-2} s^{-1}.

Diffusive O_2 fluxes within kelp-beach sediments were enhanced by two orders of magnitude compared to reference beach sediments, and the areal O_2 consumption rate is 1.4 times higher, which results in rapid depletion of O_2. During low tide, O_2 penetration was low, while during high tide O_2

penetrated the sediments by hydrodynamic forcing (Werner et al. 2006). Therefore, aerobic respiration could only occur during high tide.

The O_2 microprofiles were measured during a period with extensive kelp deposits (~0.5 m thick and covering a large part of the beach surface), and aerobic respiration rates were thus likely relatively high compared to rates during other times of the year. Based on the microbial community composition profile, the microorganisms likely responsible for fast O_2-consumption were *Bacteroidetes*, which are known to degrade complex plant- or algae-derived sugar polymers (see https://lpsn.dsmz.de, accessed on 18 July 2020) and sulfide-oxidizing *Epsilonbacteraeota*, which were present in very high relative abundances in upper sediment layers. These microbial clades showed massively increased relative sequence abundances in kelp-beach sediments compared to reference beach sediments.

Aerobic respiration can be a proxy for the sum of all mineralization processes occurring within sediments (Canfield et al. 1993), as O_2 is used in aerobic respiration and in the reoxidation of the products of anaerobic respiration (e.g., Fe^{2+}, H_2S, CH_4). In this study, this is clearly not the case. Reduced intermediates escape to the atmosphere and the sea, as evidenced by a strong sulfidic smell, the presence of sulfide oxidizers at the low tide waterline, and the occasionally high concentrations of nutrients, DOC, and sulfide in seawater. Also CH_4 is expected to escape from the sediments to the atmosphere. These reduced products of anaerobic respiration are thus not reoxidized locally by O_2 and aerobic respiration does not represent the sum of all mineralization processes.

Fe reduction

The Fe chemistry of the kelp-beach was completely different from that of the reference beach. In kelp-beach sediments, Fe(III) is converted to Fe^{2+}, which may subsequently precipitate as FeS and FeS_2. The Fe cycling is thus tightly linked to SO_4^{2-} reduction. Our extraction method does not extract the Fe(II) present as FeS_2, and the pool of Fe(II) within the sediments is thus underestimated. The absence of Fe(III) below kelp deposits points to a very strong Fe reduction potential. The regular physical forcing by storms will expose these reduced sediments to O_2 resulting in reoxidation of the Fe sulfides. Fe reduction is probably not an important process in kelp degradation, but its role as sulfide scavenger makes the process important in this environment.

SO_4^{2-} reduction

The composition of the microbial community in kelp-beach sediments appears optimized for efficient kelp degradation. The sediment below a kelp deposit as well as deeper layers of sediments next to a deposit showed increased relative proportions of SO_4^{2-} reducing deltaproteobacterial clades such as *Desulfobacterales* and *Desulfuromonadales* (see https://lpsn.dsmz.de, accessed on 18 July 2020) indicating an enhancement of SO_4^{2-} reduction induced by the kelp-derived organic material. This community composition is likely driven by regular sudden depositions of kelp, and enables rapid and efficient hydrolysis of large amounts of organic material, leading to stimulated SO_4^{2-} reduction. Only the mixing of kelp fragments into sediment, however, results in high SRR. SO_4^{2-} reduction was absent in treatments with only kelp (Table 3). Thus, the stimulation of SO_4^{2-} reduction is not driven by microorganisms on the kelp itself, but by the microbial community in kelp-beach sediments.

Consistent with bacterial distributions and the kelp deposition simulation experiments, the in situ SRR were greatly stimulated by the presence of kelp deposits. The average SRR were comparable to SRR reported for sandy intertidal sediments with high contents of organic material (Kristensen et al. 2000), but also exhibited variability in volumetric rates of up to one order of magnitude around the average (Table 3). We observed an average depletion of about 15 mmol L^{-1} SO_4^{2-} in the kelp-beach sediment porewaters relative to the reference beach (Fig. 3c). Approximately 13 d would be required to deplete SO_4^{2-} by this amount given the average SRR observed for the kelp-beach sediments. This appears to be longer than the expected residence time of porewaters for beach sediments (2–8 d) as reported for Catalina Island (Colbert et al. 2008), which is also surrounded by kelp beds. Our reported SRR may, therefore, be underestimated. The SRR were determined in October 2018, when both kelp availability and temperatures were significantly lower than in May 2018, the period of the SO_4^{2-} and sulfide measurements. Higher temperatures and availability of degradable organic material lead to higher SRR in marine surface sediments (Kristensen et al. 2000). The kelp deposition simulation experiments yielded SO_4^{2-} turnover times of only 7 d. Moreover, under conditions where sulfide oxidation can occur, especially in the presence of Fe oxides formed upon sediment oxygenation during mixing and porewater advection events (both in situ and in the incubation experiments), rapid sulfide oxidation may lead to substantial underestimation of SRR (Moeslund et al. 1994).

Methanogenesis

It is generally accepted that methanogens are outcompeted by SO_4^{2-} reducers, due to competition for H_2 and acetate (Sansone and Martens 1982). As indicated by slightly elevated CH_4 concentrations, deposition of kelp fragments, and thus degradable organic material, relieves methanogens from competition. High DOC concentrations in porewater (up to 8.9 mmol L^{-1}) show that indeed sufficient substrate is available. Supporting the occurrence of methanogenesis, we have found sequences of likely methylotrophic methanogenic *Methanolobus* archaea (see https://lpsn.dsmz.de, accessed on 18 July 2020), but only in the three deepest layers of sediment of the kelp-beach.

Aerobic respiration vs. SO_4^{2-} reduction rates

The ratio of aerobic respiration rates and SRR is relevant as aerobic processes can remove the products of anaerobic degradation, like sulfide. The uncertainty of the areal O_2 consumption rates complicates the assessment which process is most important. The aerobic processes only can occur during high tide, but SO_4^{2-} reduction continued during low tide, as SO_4^{2-} was never depleted. The estimation of the areal SRR from our measurements within the top 10 cm (3.8×10^{-7} mol m^{-2} s^{-1}) strongly underestimated the areal SRR, as SO_4^{2-} reduction occurred probably even to 1 m depth (the level of the low water line), hence the areal SRR may be underestimated by an order of magnitude. Previously, high SRR were found to occur to the level of the low water line in an intertidal sand flat, below which the rates decreased (Schutte et al. 2019). The areal SRR was 13.4 times higher than diffusive O_2 fluxes, but 4.6 times lower than areal O_2 consumption rates. However, as the areal SRR were probably about 10 times underestimated, the areal SRR may have been an order of magnitude higher than the areal O_2 consumption rates.

Also, the leakage of reduced products either next to, or through the oxygenated surface sediments, indicates that SO_4^{2-} reduction could be more important than found previously in intertidal flats and sandy beaches of the North Sea (Werner et al. 2006). We conclude that organic carbon remineralization in kelp deposits on sandy beaches is primarily driven by SO_4^{2-} reduction, and not aerobic respiration.

CO and H_2 dynamics

Higher concentrations of both CO and H_2 in kelp-beach compared to reference beach sediments indicate a production related to kelp decomposition. Our laboratory experiment showed that net CO formation from kelp mainly occurs when O_2 is available, as expected (Conrad and Seiler 1985). Therefore, the process of CO production is only of potential importance during high tide, which is when O_2 penetrates into the sediments. Net H_2 production only occurs when conditions are anoxic, thus during low tide. However, whereas CO was indeed formed under oxic conditions, it was not consumed during the subsequent anoxic phase (Fig. 6). The absence of anaerobic CO consumption indicates that the H_2 is probably not originating from CO disproportionation. Instead, the H_2 measured in the sediments is likely formed by fermentation processes. Sequences of microorganisms related to known H_2-producing fermenters like *Psychrilyobacter* (see https://lpsn.dsmz.de, accessed on 18 July 2020) were detected in increased relative abundances in kelp-beach sediments. The pathway to SRR via CO is likely not of major importance, since even if all O_2 would be used for CO production, this would not be able to fuel the very high SRR we measured.

Reduced compounds in the environment

Reduced compounds accumulate in kelp-beach sediments during low tide. During these periods of exposure, there is no advective input of oxygenated seawater. O_2 is quickly depleted, and concentrations of DOC, DIC, sulfide, S^{2-}_{tot}, N_2O, CH_4, and the nutrients NH_4^+ and P_i are high. We cannot explain the low TOC content of the kelp-beach sediment, which is almost equal to that of the reference beach sediments. The biodegradability of the TOC in kelp-beach sediment must have been much higher than that of the TOC in reference beach sediment. Although sulfide concentrations are high, they are lower than expected based on the stoichiometry of SO_4^{2-} reduction. The observed decrease of SO_4^{2-} concentrations of about 15 mmol L^{-1} would lead to the production of an equal amount of sulfide. However, sulfide concentrations reach average concentrations of about 10 mmol L^{-1}. Since we proposed that SO_4^{2-} reduction is the dominant process removing SO_4^{2-} from the porewaters, the discrepancy between SO_4^{2-} depletion and sulfide accumulation is likely caused by removal of the produced sulfide. Several processes could be responsible for the sulfide removal. One is the production of Fe sulfides, which are indeed present in elevated concentrations within kelp-beach sediments. Also, sulfide-oxidizing *Sulfurimonas*, *Sulfurovum*, and *Thiotrichaceae* occur in higher abundances within kelp-beach sediments than in reference beach sediments. Surprising is the large abundance of *Sulfurimonas* and *Sulfurovum* that are typical inhabitants of hydrothermal vent systems (Inagaki et al. 2004; Mino et al. 2017).

Sulfide that is not removed from the sediments by Fe sulfide precipitation or reoxidation escapes the sediments and reaches the atmosphere or sea. Incomplete removal of sulfide led to an intense sulfidic smell and the detection of sulfide within adjacent seawater, which enabled massive filamentous growth of sulfur-oxidizing bacteria on green algae on rocks at the low tide waterline. Surprisingly, these white filaments were not only made up of sulfur-oxidizing *Gammaproteobacteria* known from terrestrial and coastal environments (Salman et al. 2013), but also *Epsilonbacteraeota* from the family of *Sulfurovaceae*. The FISH analysis showed that both were exhibiting filamentous morphology and were growing directly next to each other. Sulfur-oxidizing *Epsilonbacteraeota* like *Sulfurovaceae* are mostly known from micro-oxic and anoxic habitats (Nakagawa et al. 2005; Meyer et al. 2013). Filamentous growth of *Sulfurovaceae* was also observed in sulfidic streams of Frassassi caves (Hamilton et al. 2015). However, in all these environments, they were found to oxidize reduced sulfur compounds via denitrification or aerobic respiration by means of high-affinity cbb3-type terminal oxidases adapted to low O_2 concentrations. The carbon fixation pathway utilized by *Epsilonbacteraeota* (reductive tricarboxylic acid cycle) is considered to be O_2 sensitive due to involvement of ferredoxins that can be oxidized easily (Campbell et al. 2006). It was very surprising to find these organisms abundantly growing on surfaces exposed to high O_2 concentrations. Remarkable is also that they have lost the genetic capacity for denitrification, which must be an adaptation to the oxic environment. Notably, the species (OTUs) forming the

white filaments did not surpass 1% relative abundance in the sediments. Instead, sediment samples were dominated by other *Sulfurovaceae* species, which are probably more adapted to low O_2 environments.

Kelp deposition enriches a rare sulfur-oxidizing *Sulfurovaceae* species adapted to oxic environments. A brief analysis of the genomic potential and comparison to other *Sulfurovaceae* genomes showed that the genomes of filament-forming *Sulfurovaceae* populations encoded low-affinity aa3-type terminal oxidases absent from the vast majority of reference genomes. As also no denitrification genes were found, these filament-forming *Sulfurovaceae* species are adapted to aerobic respiration at high O_2 concentrations. A gene unique to the Helgoland genomes was encoding an anti-oxidative protein, hinting at further unique adaptation to high O_2 levels. All denitrification genes (e.g., for nitric- and nitrous-oxide reductases) found in the metagenome were associated to *Gammaproteobacteria*. However, the Helgoland *Sulfurovum* genomes encoded a NO-detoxifying dioxygenase. This might be a hint that although they cannot denitrify themselves, they might be adapted to co-exist with NO-evolving incomplete denitrifyers.

The microbial community composition showed clear stratification by depth only in the kelp-beach sediments, yet not underneath the deposits themselves. As typically in sediments, the microbial community stratification seems to reflect the different O_2 levels with SO_4^{2-} reducers and anaerobic organisms more abundant in the lower and sulfide oxidizers and aerobic microorganisms more abundant in the upper layers. While the lack of stratification at the reference beach is likely caused by high permeability and resulting oxygenation of the sediment combined with low respiration rates, underneath the kelp the lack of stratification is likely caused by the lack of O_2 penetrating the sediment from above.

Further research is needed in order to elucidate the main substrates for SO_4^{2-} reducers. One of the steps would be to focus on obtaining a more detailed view of the heterotrophic microorganisms associated with kelp-beach sediments, and investigate who are the specialized kelp degraders present. It would furthermore be of importance to find the hydrolysis products, and test their effects on aerobic respiration and SO_4^{2-} reduction.

Conclusions

Although sandy beaches are very dynamic systems with fast and large changes in hydration, temperature and salinity, the intense degradation of kelp deposits leads to distinct changes in biogeochemical conditions and microbial community composition in the underlying sandy sediments. The major processes driving these changes are highly increased fermentation and SO_4^{2-} reduction. We found that the sum of degradation processes in sandy sediments is not reflected in the total respiration rate, as these sediments are an open system where reduced compounds are washed out before they are completely oxidized. The export of intermediates and sulfide from kelp deposits leads to a spatial separation of SO_4^{2-} reduction and sulfide oxidation. The described conditions select for a microbial community composition that is highly optimized for degradation of large amounts of kelp. It is ready to instantly start kelp degradation and able to efficiently utilize the resulting large amounts of reduced compounds.

References

Berner, R. A. 1980. Early diagenesis: A theoretical approch. Princeton Univ. Press.

Böttcher, M. E., A. Rusch, T. Höpner, and H.-J. Brumsack. 1997. Stable sulfur isotope effects related to local intense sulfate reduction in a tidal sandflat (southern North Sea): Results from loading experiments. Isotopes Environ. Health Stud. **33**: 109–129. doi:10.1080/10256019808036363

Campbell, B. J., A. S. Engel, M. L. Porter, and K. Takai. 2006. The versatile ε-proteobacteria: Key players in sulphidic habitats. Nat. Rev. Microbiol. **4**: 458–468. doi:10.1038/nrmicro1414

Canfield, D. E. et al. 1993. Pathways of organic carbon oxidation in three continental margin sediments. Mar. Geol. **113**: 27–40, doi: 10.1016/0025-3227(93)90147-N

Chen, J. and others. 2017. Impacts of chemical gradients on microbial community structure. ISME J. **11**: 920–931, doi: 10.1038/ismej.2016.175

Cline, J. D. 1969. Spectrophotometric determination of hydrogen sulfide in natural waters. Limnol. Oceanogr. **14**: 454–458. doi:10.4319/lo.1969.14.3.0454

Colbert, S. L., W. M. Berelson, and D. E. Hammond. 2008. Radon-222 budget in Catalina Harbor, California: 2. Flow dynamics and residence time in a tidal beach. Limnol. Oceanogr. **53**: 659–665. doi:10.4319/lo.2008.53.2.0659

Colombini, I., A. Aloia, M. Fallaci, G. Pezzoli, and L. Chelazzi. 2000. Temporal and spatial use of stranded wrack by the macrofauna of a tropical sandy beach. Mar. Biol. **136**: 531–541. doi:10.1007/s002270050713

Colombini, I., and L. Chelazzi. 2003. Influence of marine allochthonous input on sandy beach communities. Oceanogr. Mar. Biol. Annu. Rev. **41**: 115–159.

Conrad, R., and W. Seiler. 1985. Characteristics of abiological carbon monoxide formation from soil organic matter, humic acids, and phenolic compounds. Environ. Sci. Technol. **19**: 1165–1169. doi:10.1021/es00142a004

Dugan, J. E., D. M. Hubbard, H. M. Page, and J. P. Schimel. 2011. Marine macrophyte wrack inputs and dissolved nutrients in beach sands. Estuaries Coasts **34**: 839–850. doi:10.1007/s12237-011-9375-9

Duggins, D. O., C. A. Simenstad, and J. A. Estes. 1989. Magnification of secondary production by kelp detritus in coastal marine ecosystems. Science **245**: 170–173. doi:10.1126/science.245.4914.170

Froelich, P. N., and others. 1979. Early oxidation of organic matter in pelagic sediments of the eastern equatorial Atlantic: Suboxic diagenesis. Geochim. Cosmochim. Acta **43**: 1075–1090. doi:10.1016/0016-7037(79)90095-4

Grasshoff, K., K. Kremling, and M. Ehrhardt. 1999. Methods of seawater analysis. New York: Wiley.

Hall, P. O. J., and R. C. Aller. 1992. Rapid, small-volume, flow injection analysis for ΣCO_2, and NH_4^+ in marine and freshwaters. Limnol. Oceanogr. **37**: 1113–1119. doi:10.4319/lo.1992.37.5.1113

Hamilton, T. L., D. S. Jones, I. Schaperdoth, and J. L. Macalady. 2015. Metagenomic insights into S(0) precipitation in a terrestrial subsurface lithoautotrophic ecosystem. Front. Microbiol. **5**: 756. doi:10.3389/fmicb.2014.00756

Inagaki, F., K. Takai, K. H. Nealson, and K. Horikoshi. 2004. *Sulfurovum lithotrophicum* gen. nov., sp. nov., a novel sulfur-oxidizing chemolithoautotroph within the *ε-Proteobacteria* isolated from Okinawa trough hydrothermal sediments. Int. J. Syst. Evol. Microbiol. **54**: 1477–1482. doi:10.1099/ijs.0.03042-0

Jeroschewski, P., C. Steuckart, and M. Kühl. 1996. An amperometric microsensor for the determination of H_2S in aquatic environments. Anal. Chem. **68**: 4351–4357. doi:10.1021/ac960091b

Jickells, T. D., and J. E. Rae. 1997. Biogeochemistry of intertidal sediments, p. 1–15. *In* T. D. Jickells and J. E. Rae [eds.], Biogeochemistry of intertidal sediments. Cambridge University Press.

Jørgensen, B. B. 1982. Mineralization of organic matter in the sea bed—The role of sulphate reduction. Nature **296**: 643–645. doi:10.1038/296643a0

Koop, K., and J. G. Field. 1980. The influence of food availability on population dynamics of a supralittoral isopod, *Ligia dilatata* brandt. J. Exp. Mar. Biol. Ecol. **48**: 61–72. doi:10.1016/0022-0981(80)90007-6

Koop, K., and C. L. Griffiths. 1982. The relative significance of bacteria, meio- and macrofauna on an exposed sandy beach. Mar. Biol. **66**: 295–300. doi:10.1007/BF00397035

Koop, K., R. C. Newell, and M. I. Lucas. 1982. Biodegradation and carbon flow based on kelp (*Ecklonia maxima*) debris in a sandy beach microcosm. Mar. Ecol. Prog. Ser. **7**: 315–326. doi:10.3354/meps007315

Kristensen, E., J. Bodenbender, M. H. Jensen, H. Rennenberg, and K. M. Jensen. 2000. Sulfur cycling of intertidal Wadden Sea sediments (Konigshafen, Island of Sylt, Germany): Sulfate reduction and sulfur gas emission. J. Sea Res. **43**: 93–104. doi:10.1016/S1385-1101(00)00007-1

Kühl, M., R. N. Glud, H. Ploug, and N. B. Ramsing. 1996. Microenvironmental control of photosynthesis and photosynthesis-coupled respiration in an epilithic cyanobacterial biofilm. J. Phycol. **32**: 799–812. doi:10.1111/j.0022-3646.1996.00799.x

Li, Y.-H., and S. Gregory. 1974. Diffusion of ions in sea water and in deep-sea sediments. Geochim. Cosmochim. Acta **38**: 703–714. doi:10.1016/0016-7037(74)90145-8

Mann, K. H. 1973. Seaweeds: Their productivity and strategy for growth. Science **182**: 975–981. doi:10.1126/science.182.4116.975

Manz, W., R. Amann, W. Ludwig, M. Wagner, and K.-H. Schleifer. 1992. Phylogenetic oligodeoxynucleotide probes for the major subclasses of proteobacteria: Problems and solutions. Syst. Appl. Microbiol. **15**: 593–600. doi:10.1016/S0723-2020(11)80121-9

Meier, D. V., P. Pjevac, W. Bach, S. Hourdez, P. R. Girguis, C. Vidoudez, R. Amann, and A. Meyerdierks. 2017. Niche partitioning of diverse sulfur-oxidizing bacteria at hydrothermal vents. ISME J. **11**: 1545–1558. doi:10.1038/ismej.2017.37

Meyer, J. L., N. H. Akerman, G. Proskurowski, and J. A. Huber. 2013. Microbiological characterization of post-eruption "snowblower" vents at axial seamount, Juan de Fuca ridge. Front. Microbiol. **4**: 153. doi:10.3389/fmicb.2013.00153

Millero, F. J., T. Plese, and M. Fernandez. 1988. The dissociation of hydrogen sulfide in seawater. Limnol. Oceanogr. **33**: 269–274. doi:10.4319/lo.1988.33.2.0269

Mino, S. and others. 2017. Endemicity of the cosmopolitan mesophilic chemolithoautotroph *Sulfurimonas* at deep-sea hydrothermal vents. ISME J **11**: 909–919, doi: 10.1038/ismej.2016.178

Moeslund, L., B. Thamdrup, and B. B. Jørgensen. 1994. Sulfur and iron cycling in a coastal sediment: Radiotracer studies and seasonal dynamics. Biogeochemistry **27**: 129–152. doi:10.1007/BF00002815

Nakagawa, S., K. Takai, F. Inagaki, H. Hirayama, T. Nunoura, K. Horikoshi, and Y. Sako. 2005. Distribution, phylogenetic diversity and physiological characteristics of epsilon-*Proteobacteria* in a deep-sea hydrothermal field. Environ. Microbiol. **7**: 1619–1632. doi:10.1111/j.1462-2920.2005.00856.x

Parshina, S. N., J. Sipma, A. M. Henstra, and A. J. M. Stams. 2010. Carbon monoxide as an electron donor for the biological reduction of sulphate. Int. J. Microbiol. **2010**: 319527–319529. doi:10.1155/2010/319527

Pehlke, C., and I. Bartsch. 2008. Changes in depth distribution and biomass of sublittoral seaweeds at Helgoland (North Sea) between 1970 and 2005. Climate Res. **37**: 135–147. doi:10.3354/cr00767

Robbins, L. L., M. E. Hansen, J. A. Kleypas, and S. C. Meylan. 2010. CO2calc: A user-friendly seawater carbon calculator for Windows, Mac OS X, and iOS (iPhone). U.S. Geological Survey Open-File Report: 2010–1280, p. 17.

Rodil, I. F., M. Lastra, J. López, A. P. Mucha, J. P. Fernandes, S. V. Fernandes, and C. Olabarria. 2019. Sandy beaches as biogeochemical hotspots: The metabolic role of macroalgal wrack on low-productive shores. Ecosystems **22**: 49–63. doi:10.1007/s10021-018-0253-1

Røy, H., H. S. Weber, I. H. Tarpgaard, T. G. Ferdelman, and B. B. Jørgensen. 2014. Determination of dissimilatory sulfate reduction rates in marine sediment via radioactive ^{35}S tracer. Limnol. Oceanogr. Methods **12**: 196–211. doi:10.4319/lom.2014.12.196

Salman, V., J. V. Bailey, and A. Teske. 2013. Phylogenetic and morphologic complexity of giant sulphur bacteria. Antonie Van Leeuwenhoek **104**: 169–186. doi:10.1007/s10482-013-9952-y

Sansone, F. J., and C. S. Martens. 1982. Volatile fatty acid cycling in organic-rich marine sediments. Geochim. Cosmochim. Acta **46**: 1575–1589. doi:10.1016/0016-7037(82)90315-5

Schutte, C. A., S. Ahmerkamp, C. S. Wu, M. Seidel, D. de Beer, P. L. M. Cook, and S. B. Joye. 2019. Biogeochemical dynamics of coastal tidal flats, p. 407–440. *In* G. M. E. Perillo, E. Wolanski, D. R. Cahoon, and C. S. Hopkinson [eds.], Coastal wetlands: An integrated ecosystem approach. Elsevier.

Siegismund, F., and C. Schrum. 2001. Decadal changes in the wind forcing over the North Sea. Climate Res. **18**: 39–45. doi:10.3354/cr018039

Soetaert, K., A. F. Hofmann, J. J. Middelburg, F. J. R. Meysman, and J. Greenwood. 2007. The effect of biogeochemical processes on pH. Mar. Chem. **105**: 30–51. doi:10.1016/j.marchem.2006.12.012

Treude, T., C. R. Smith, F. Wenzhöfer, E. Carney, A. F. Bernardino, A. K. Hannides, M. Krüger, and A. Boetius. 2009. Biogeochemistry of a deep-sea whale fall: Sulfate reduction, sulfide efflux and methanogenesis. Mar. Ecol. Prog. Ser. **382**: 1–21. doi:10.3354/meps07972

Uhl, F., I. Bartsch, and N. Oppelt. 2016. Submerged kelp detection with hyperspectral data. Remote Sens. (Basel) **8**: 487. doi:10.3390/rs8060487

Usov, A. I., G. P. Smirnova, and N. G. Klochkova. 2001. Polysaccharides of algae: 55. Polysaccharide composition of several brown algae from Kamchatka. Russ. J. Bioorg. Chem. **27**: 395–399. doi:10.1023/A:1012992820204

Viollier, E., P. W. Inglett, K. Hunter, A. N. Roychoudhury, and P. van Cappellen. 2000. The ferrozine method revisited: Fe(II)/Fe(III) determination in natural waters. Appl. Geochem. **15**: 785–790. doi:10.1016/S0883-2927(99)00097-9

von Haugwitz, W., H. K. Wong, and U. Salge. 1988. The mud area southeast of Helgoland: A reflection seismic study. Mitt. Geol.-Paläont. Inst. Univ. Hamburg **65**: 409–422.

Werner, U., M. Billerbeck, L. Polerecky, U. Franke, M. Huettel, J. E. E. van Beusekom, and D. de Beer. 2006. Spatial and temporal patterns of mineralization rates and oxygen distribution in a permeable intertidal sand flat (Sylt, Germany). Limnol. Oceanogr. **51**: 2549–2563. doi:10.4319/lo.2006.51.6.2549

Acknowledgments

We thank the technical assistants of the Microsensor group at the MPI Bremen for microsensor construction and general lab assistance, and Katrin Knittel and Sebastian Miksch for their help with the procedures for total cell counting. Martina Alisch is thanked for the DIC and nutrient measurements. Jenny Wendt is thanked for TOC measurements at the MARUM. Matija Lagator and Marwa Baloza are thanked for field and laboratory assistance. Further we would like to thank Prof. Rudolf Amann for his generous support of the project and the Max Planck Genome Centre Cologne for sequencing. We thank Jesse McNichol for kindly providing *Sulfurovum* FISH probes. The staff of the Biological Station Helgoland is thanked for their hospitality and provision of their facilities. The discovery of white mats was made during a field course of the MarMic Masters program of MPI Bremen and initial collection of biofilm material was performed by the students of MarMic class 2020. We are grateful for the constructive comments of the two anonymous reviewers. This study was funded by the Max Planck Institute for Marine Microbiology should be replaced by Max Planck Society. Open access funding enabled and organized by Projekt DEAL.

Conflict of Interest

None declared.

Submitted 17 January 2020
Revised 09 June 2020
Accepted 14 July 2020

Associate editor: Ronnie Glud